REAL-TIME MODELS OF VALVE SOLENOIDS: AN EVALUATION OF MEASUREMENT AND SIMULATION-BASED PARAMETER IDENTIFICATION

Simon Hucko[1]*, Xiaosha Tao[1], Katharina Schmitz[1]

[1]*Institute for Fluid Power Drives and Systems, RWTH Aachen University, Campus-Boulevard 30, 52074 Aachen*

* Corresponding author: Tel.: +49 241 80 47744; E-mail address: simon.hucko@ifas.rwth-aachen.de

ABSTRACT

This paper examines the challenges of real-time modeling solenoid valve actuators. Usually, more complex real-time models are executed as lumped parameter models, often simulatively parameterized, using finite element method (FEM) models. The quality of the simulative parameterization heavily depends on the accuracy of the FEM model. The accuracy, in turn, is largely determined by the material parameters used to create the FEM simulation. Variations within the material can render the primary material parameters inaccurate, thereby reducing the accuracy of the FEM model and consequently the derived parameters. The quality of the real-time model thus largely depends on the quality of the material parameters.

To eliminate uncertainties introduced by subpar material parameters and to enable precise real-time models, this work showcases the possibility to reconstruct required material parameters simulatively from flux measurements. The more accurate material data obtained using this new approach could also improve the accuracy when adapting components to new requirements. The paper describes a model with lumped parameters, as well as an FEM simulation model, a test rig, and the process of B(H)/initial magnetization curve calculation, followed by validation with new operating conditions.

Keywords: Model Based Development, Softsensor, Solenoid, Valve

1. INTRODUCTION

1.1. Motivation

For decades, solenoids have been widely used as valve actuators in fluid power technology, due to their low manufacturing costs, high force density, speed and efficiency. Growing demands on functionality and the quest for better control account for the need for more detailed modeling of actuators. Applications include model-based design, condition monitoring, and the acquisition of additional data through soft sensors [1]. However, most of these applications require an accurate and comprehensive real-time model of the considered system.

1.2. Challenge and Approach

As part of the modeling process, it is necessary to find numerical representations for various coupled effects of the electrical, magnetic and mechanical domains of the solenoid, as these have significant influence on system behavior. A particular challenge is posed by the nonlinearities of the electromagnetic subsystem. In general, the nonlinearities can be categorized into rate-independent effects, such as magnetic hysteresis, and rate-dependent effects, such as eddy currents or friction [2].

In order to enable broad application, it is necessary to not only create a suitable representation of the effects, but also a cost-effective parameterization. Additionally, the models must be computable on common microprocessors within the given cycle time. Magnetic hysteresis in particular is often neglected due to the time required to parameterize mathematical hysteresis models. There are several main options for electromagnetic modeling, such as the use of black-box models, FEM-driven models, or analytical models with lumped parameters. The latter option is far less complex than the others and can be used in control applications as, for example, in model-based valve controls [3–5]. The models used can be parameterized with the help of measurements as shown in [3]. Due to the required complexity of comprehensive data acquisition and processing, such models are increasingly parameterized with simulated data. Parameterization often relies on data from magnetostatic FEM simulation-models [6]. The accuracy of these FEM models is highly dependent on the material parameters, which are usually provided by the solenoid manufacturers or material suppliers. However, uncertainties in material parameters arise from steel processing as well as variations within production batches, making it difficult to estimate the accuracy of characteristics derived from FEM models [7]. An independent determination of the assembled magnet's material parameters or initial magnetization curve is thus advisable. However, even if all flux-carrying parts of the magnetic circuit are made of the same material, it is often not feasible to analytically determine the initial curve from the measured excitation current and the magnetic flux generated by the actuator coil.

The aim of this work is therefore to investigate the possibility of simulatively reconstructing the initial magnetization curve with flux measurements, which were recorded using the assembled solenoid. By implementing an optimization algorithm, taking into account physical constraints, the initial curve is adjusted in such a way that the simulated magnetic flux converges to the measured magnetic flux.

This novel approach is validated in multiple steps: First, different operating points are simulated with the newly determined material parameters using the FEM model. The results are then compared to measured data. Subsequently, parameters for a real-time capable actuator model are derived from the FEM model. The results of the actuator model using non optimized parameters and those generated using optimized parameters are in turn compared with measurement data.

1.3. Structure of the Paper

The present study is structured as follows: First, a lumped-parameter model of a valve actuator is described. Then, the test rig for the metrological investigation of magnetic actuators is presented. Next, the structure of an FEM simulation model of an exemplarily considered actuator is explained. This FEM model is then used in conjunction with the measurement results to calculate the initial curve and parameters for a real-time capable model are derived. Finally, the simulation is validated and compared to measured data.

2. MODELING OF VALVE SOLENOIDS

In this section, the design of a lumped-parameter and an FEM model is described. The actuator under consideration is a commercially available proportional solenoid which is used in hydraulic control valves of nominal size 6. The sectional view of the solenoid can be seen in **Figure 1**.

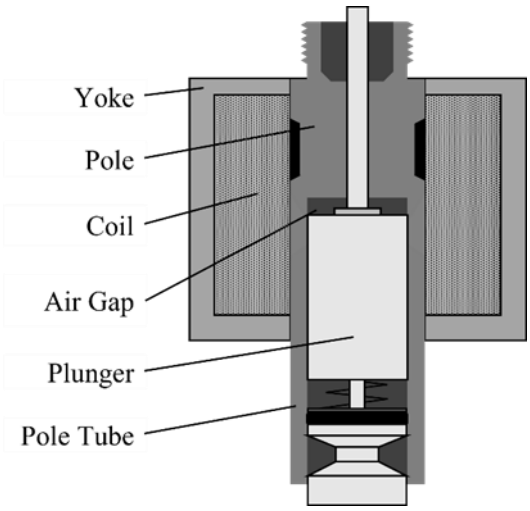

Figure 1: Sectional View of a Proportional Valve Solenoid

2.1. Lumped-Parameter Model

Lumped-parameter models are simplified mathematical representations in which the spatial distribution of the system is neglected. It is assumed that all components of the system are concentrated in one point. This reduces the partial differential equations describing the system to a topology or ordinary differential equations.

For modeling, the considered system is commonly divided into different domains. In case of solenoids, usually the electrical, the magnetic and the mechanical domains are taken into account. Each domain itself is represented by a network of discrete interconnected elements with concentrated parameters.

These elements are interconnected by system equations, enabling the simulation of the solenoid's response to various input signals.

The electrical system can be described by Equation 1, where U is the voltage applied to the coil, which is equal to the sum of the voltage across the winding resistor R and the induction voltage [8]. The magnetic system can be described by Equation 2. The magnetomotive force Θ constitutes the sum of the field-generating current i_f and the eddy current i_{eddy}. The field-generating current i_f corresponds to the product of the magnetic resistance R_m and Ψ. When modeling the eddy currents in a simplified way by assuming a constant flux distribution, i_{eddy} can be calculated from the eddy current parameter L_{eddy} and the induction voltage [8]. w equals the number of the coil's windings, i is the electric current, and Ψ the flux linkage. According to [8], the force generated by the solenoid depends on the flux linkage and on the position of the armature x, as described in Equation 3. For simplification, the generated force as well as the field-generating current are approximated by a characteristic map dependig on Ψ and x in the further course. For the calculation of the eddy currents, they are assumed to be proportional to the induction voltage.

$$U = R \cdot i + \frac{d\Psi}{dt} \tag{1}$$

$$\Theta = w^2 \cdot i = \Psi \cdot R_m + L_{eddy} \frac{d\Psi}{dt} \tag{2}$$

$$\mathrm{F_m} = \frac{\mathrm{d}}{\mathrm{dx}} \int_{\mathrm{I_0}}^{0} \Psi \, \mathrm{di} \tag{3}$$

By using these equations, the simple, computationally inexpensive solenoid model shown in **Figure 2** can be formulated.

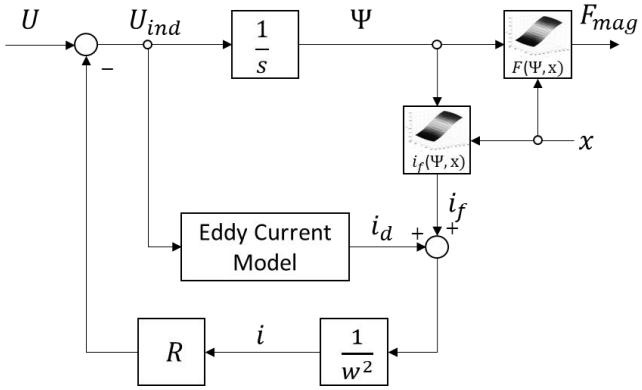

Figure 2: Lumped Network Solenoid Model.

2.2. Finite-Element-Modeling

Finite element modeling is a numerical simulation technique which divides the solenoid into small elements and calculates the electromagnetic field interactions within each element. FEM models provide a detailed and accurate representation of the solenoid's behavior, accounting for complex geometries and materials. They can simulate both static and dynamic responses of the solenoid, including factors like magnetic saturation and eddy current losses.

Solenoid valve actuators typically feature rotational axisymmetry, making 2D axisymmetric FEM simulations cost-effective. However, some plungers/armatures introduce non-axisymmetric elements. For example, in fluid-filled pole tubes, the armature is provided with round or rectangular channels. These prevent or reduce a pressure-induced counterforce when the armature moves. In the exemplarily considered magnet, the fluid is equalized by two holes in the plunger. Such non-rotationally symmetric elements can be transformed into an equivalent rotationally symmetric geometry. This requires the iron cross-section effective for the magnetic flux to remain the same [5, 8].

To allow for an automated multiple execution of the model in a manageable time, a parameterized 2D model of the considered magnet was created. The model should allow the variable adjustment of the armature displacement and the excitation current. **Figure 3** shows the 2D solenoid model and meshing.

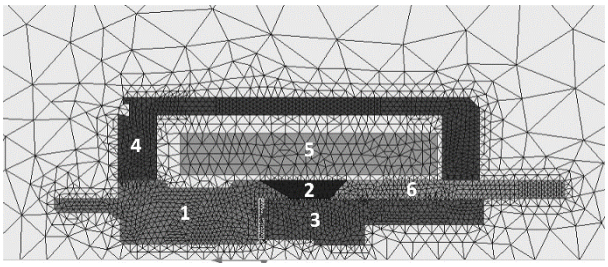

Figure 3: 2D FEM Model, 1. Pole, 2. Non-Magnetizable Area, 3. Plunger, 4. Yoke, 5. Coil, 6. Pole Tube.

The coil has an orthocyclic winding. In order to calculate the fill factor of the coil, the area of the conductor was divided by the area of the winding [8].

A variable air gap as shown in **Figure 1**, was implemented to account for the armature movement. In the area of the air gap, the automatically generated mesh was manually revised to increase precision. The non-magnetic area between pole and pole tube has been simulated as air.

The non-magnetic area between pole and pole tube as well as between pole and armature was simulated as air. A polytetrafluoroethylene sheet is used between the armature and the pole tube to reduce friction. To determine the parasitic air gap between the plunger and the pole tube, the diameter of the plunger and that of the pole tube were measured and subtracted from each other. The same has been done for the air gap between yoke and pole and between yoke and pole tube. Parts 1,3,4 and 6 are part of the flux-carrying iron circuit made of the same soft magnetic material. Material properties were added manually using data from manufacturers, material producers, or actual measurements.

The 2D model allows to calculate the force generated by the actuator under various current levels and armature strokes as well as the magnetic flux magnitude under different currents.

2.3. Nonlinear Material Characteristics

Soft magnetic materials are used for electromagnetic actuators. They are characterized by a narrow hysteresis curve and thus low hysteresis losses during magnetization.

The initial magnetization of the material follows the so-called initial curve depicted in **Figure 4**. The proportionality factor μ between the magnetic flux density B and the magnetic field strength H is called permeability. The permeability describes the slope of the B(H)curve and characterizes the influence of different materials on the magnetic field.

With the relative permeability μ_r, the absolute permeability can be expressed as a multiple of the induction constant μ_0. Beyond the saturation flux density B_S, the B(H) behaves linearly and approaches μ_0 [8].

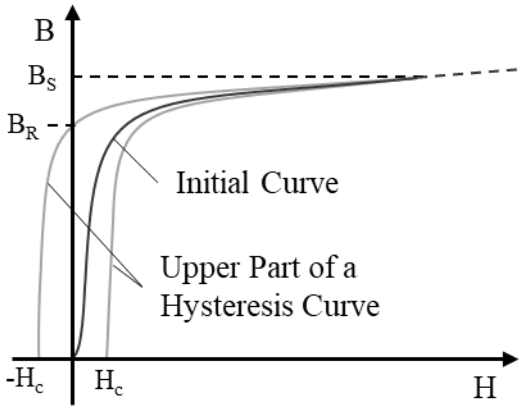

Figure 4: B(H) Characteristic Curve with Initial Curve.

3. TEST RIG

The test rig described below is used to investigate solenoids. For the present work, the magnetic flux and force generated by the solenoid were determined at different excitations and positions.

The setup shown in **Figure 5** and **Figure 6** was designed to allow for precise measurement of a wide variety of valve solenoids. **Figure 5** shows the mechanical part of the test rig.

On the left side, the test-solenoid is mounted on a rigid frame. A movable carriage driven by a servo motor allows for precise, dynamic positioning of a mechanical stop against which the armature presses. The force generated by the armature is recorded by a force sensor (MES-KM40). Both the position of the armature and the position of the carriage are measured to precisely control the armature position and to eliminate possible position deviations, for example due to backlash or the limited stiffness of the force sensor.

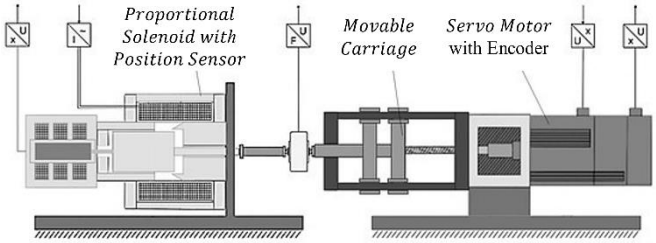

Figure 5: Schematic Depiction of the Mechanical Setup for Measuring Solenoids [1].

In **Figure 6**, the electrical part of the experimental setup is schematically shown. The circuit consists of the solenoid itself, an amplifier and a low-side measurement shunt (3 Ω ± 0.02%) for current measurement.

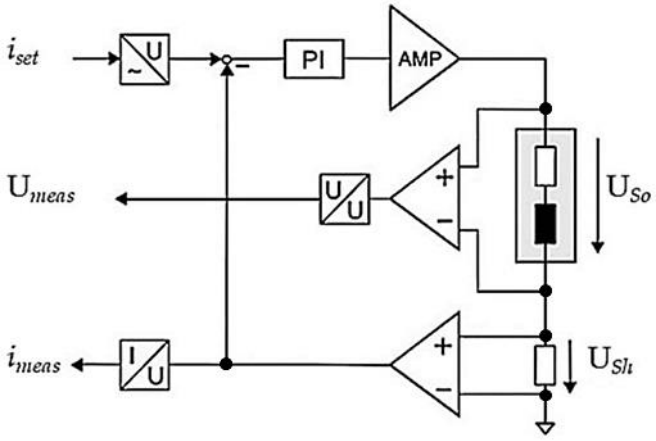

Figure 6: Electrical Schematic for Measuring Solenoids [1].

The amplifier (Kikusuiu PBZ80-5) allows, in push/pull configuration, the application of arbitrary currents and voltages. The solenoid is highlighted by a grey rectangle and is represented by an inductor and an ohmic resistor. The temperature change in the measurement shunt is small due to sufficient cooling. The resulting change in resistance is therefore negligible. The voltage is measured across the solenoid. The synchronized acquisition of voltage, current and force is carried out using a measuring amplifier (MC USB 404-60).

The flux is calculated according to Equation 4 using the measured voltage U and the current i.

$$\Psi(x,i) = \int_0^t (U - R \cdot i)\ dt \tag{4}$$

The flux curves determined in this way are shown in **Figure 7** for excitations of 0.5 A, 1 A and 1.5 A.

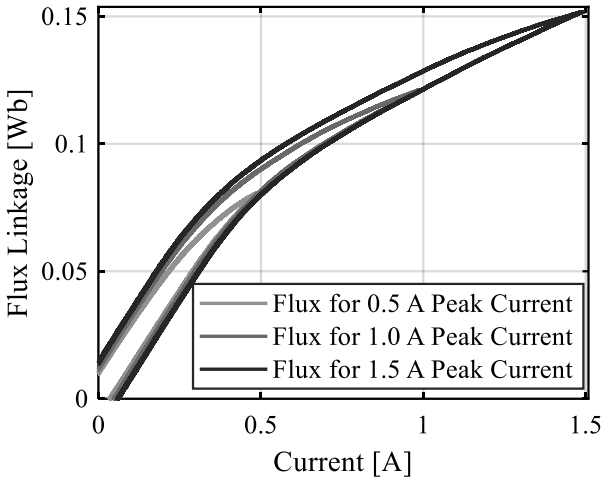

Figure 7: Measured Flux Characteristics of a Solenoid for a Triangular Excitation with a Peak Current of 0.5 A, 1.0 A and 1.5 A at a Stroke of 1.5 mm.

The measured force characteristics are shown in **Figure 8**. In order to avoid static friction at a constant current, the armature was moved quasi-statically between the stops using the servo motor shown in **Figure 5**. The position was detected using the actuator's own position sensor.

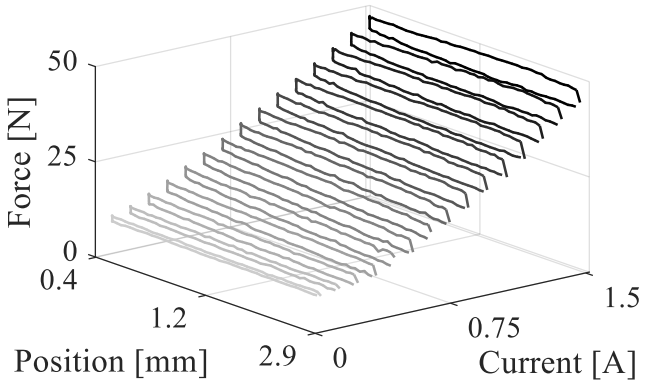

Figure 8: Measured Force Characteristics of a Solenoid.

The equally shaded lines on top of each other represent the force progression with ascending and descending directions of movement for each current step. The force hysteresis is clearly visible. The solenoid's air gap is reduced with decreasing voltage of the position sensor. Without using a dither signal, the force hysteresis for this solenoid is 1–5 N. However, modeling this relationship would exceed the scope of this paper. Therefore, the individually recorded hysteresis curves were averaged and interpolated, providing the magnetic force for a given current and position.

4. NEW METHOD FOR B/H CURVE ESTIMATION

To simulate magnetic actuators, common FE programs use initial magnetization curves (henceforth referred to as initial curve) up to saturation to account for nonlinear material characteristics.

The initial curve is practically identical with the commutation curve which can be constructed from completely recorded hysteresis curves [9]. Considering a sample with simple geometry and homogeneous flux density, the hysteresis curves and from them the initial curve can be determined by measuring the magnetic flux and the electric current using Equations 5 and 6.

$$\oint_l H\, dl = \sum I = w \cdot I \tag{5}$$

$$\Phi = \int_A B\ dA \tag{6}$$

Due to the complex geometry of a valve solenoid as well as the inconsistent flux density and field strength, the previously described procedure is not applicable. Even though the iron/magnetic circuit can be broken down into a number of simpler sub geometries, the respective magnetic field strengths and flux densities of these sub geometries are usually unknown. A simple calculation is therefore not feasible.

The new method presented in the following, enables the determination of an initial curve from measured flux/current curves by coupling an FEM program with an optimizer.

4.1. Idea of the Optimization Procedure

Using an initial curve from literature and a given valve solenoid geometry, a FEM simulation can be performed. This simulation calculates the magnetic flux for an entered excitation. Subsequently, the difference or error between the simulated magnetic flux and the measured flux is calculated as given in Equation 7, where n represents the number of measurement points or simulations.

$$e = \frac{1}{n} \cdot \sum_{i=1}^{n} \sqrt{\left(\Psi mess(i)\right)^2 - \left(\Psi sim(i)\right)^2} \tag{7}$$

If the accuracy of the measurement, the geometric dimensions and the quality of the meshing are appropriate, this error can be attributed to the initial curve used for simulation. Consequently, the error can be reduced by adjusting the initial curve. Hence, the main objective of this method is to reconstruct the initial curve of the material from measured magnetic fluxes. This reconstruction is done by iteratively performing static FEM simulations of the magnet. In each step, the calculated magnetic flux is compared to the measured one to calculate the error. With the help of an optimizer, the initial curve is then adjusted to reduce the error. This optimization is performed at a fixed armature position for different excitations.

4.2. Optimization

Figure 9 shows the conceptual structure of the optimization.

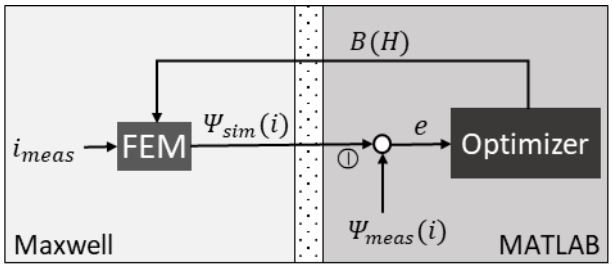

Figure 9: Block Diagram of the Optimization Procedure.

The algorithm used for the procedure forms a feedback loop which enables adaptive automated simulations through the integration of ANSYS Maxwell and MATLAB. As far as the authors are aware, there is no direct interface between MATLAB and ANSYS Maxwell allowing such an optimization. Therefore, a suitable interface was developed to facilitate the required data transfer.

In **Figure 9** the left side represents the simulations of the FEM model in ANSYS Maxwell, while the right side illustrates the optimization algorithm developed in MATLAB.

The initial curve, once optimized, is returned to the FEM simulation model in the form of a data table. Within the FEM simulation model, the new curve and equivalent measured excitation current i_{mess} are used to calculate new magnetic fluxes $\Psi_{sim}(i)$. Subsequently, $\Psi_{sim}(i)$ is passed back to MATLAB, where the error e is calculated. This process iterates automatically until the specified optimization conditions are met, for example by reaching a maximum number of computation cycles or by achieving the required accuracy.

In the following, the selection of the optimization algorithm is explained.

The definition of favorable boundary and initial conditions can help to minimize the number of necessary iteration steps. The chosen conditions, the resulting requirements for the algorithm and the choice of the algorithm are explained.

As depicted in **Figure 9**, the initial curve is the output parameter of the MATLAB module and serves as the optimization objective. The input parameter is the magnetic flux $\Psi_{sim}(i)$, derived from the FEM calculation. The error function to be optimized, is defined by Equation 7.

As defined in [8], the initial magnetization curve shown in **Figure 4** exhibits nonlinear, steadily increasing properties.

The curve has an inflection point, prior to which the permeability increases strictly monotonically. After the inflection point, it decreases strictly monotonically, until complete saturation. When exceeding the saturation flux density, the initial curve behaves linearly and approaches μ_0.

Based on these characteristics, constraints on the optimized curve are established.

Aside from introducing constraints, the number of iterations can be reduced by choosing suitable starting parameters. Typically, there is reference data available for the initial curve to be optimized, provided by literature, the manufacturer or material supplier.

To summarize, when selecting an algorithm to minimize the error function, the following aspects must be considered:

- Nonlinearity of the optimized parameter
- Possibility to define initial values
- Ability to set continuity conditions or create nonlinear constraints

Based on the given requirements, the augmented Lagrangian pattern search algorithm was selected. The pattern search method is an optimization algorithm which does not require derivatives of the objective function during computation. The augmented Lagrangian method is a mathematical optimization technique commonly used in pattern search algorithms. It addresses constrained optimization problems, where both equality and inequality constraints exist. It does so by introducing a penalty term into the objective function, which quantifies the violation of constraints and adjusts this penalty based on Lagrange multipliers. The method iteratively optimizes the augmented Lagrangian function, gradually reducing the constraint violations. The process allows the algorithm to search for optimal solutions while accounting for constraints.

4.3. Evaluation of Results

The aim of the optimization is to minimize the error between the measured and simulated fluxes. **Figure 10** shows the measured magnetic flux and the flux calculated with the FEM model for a piston stroke of 1.0 mm. After optimization, the two lines essentially coincide.

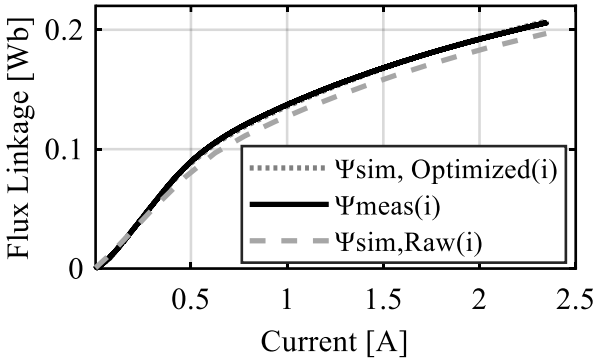

Figure 10: Comparison of Measured $\Psi_{\mathrm{meas}}(\mathrm{i})$, $\Psi_{\mathrm{sim,Optimized}}(\mathrm{i})$ with the Optimized and $\Psi_{sim,Raw}(\mathrm{i})$ with the Unoptimized Initial Curve at 1.0 mm Stroke.

Figure 11 shows the initial curve of the material used. The dashed line is the original, non-optimized curve. It was obtained from the work of [7] and served as a starting point for the optimization.

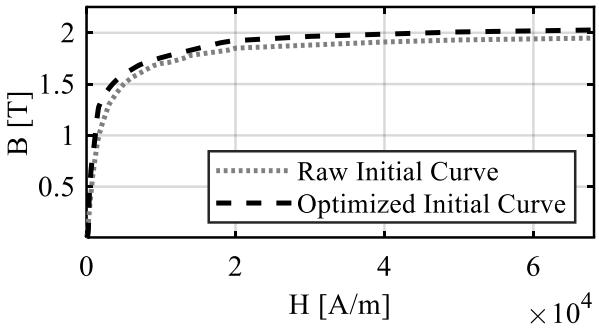

Figure 11: Unoptimized (Dotted) and Optimized (Dashed) Initial Magnetization Curve.

After about two thousand iteration steps, the initial curve, shown as a solid line in **Figure 11,** is obtained. It is evident, that saturation of the optimized curve occurs at higher field strengths.

5. EVALUATION OF SIMULATION-BASED PARAMETER ESTIMATION FOR REAL-TIME MODELS

To parameterize the model shown in **Section 2**, $F(\Psi, x)$, $i_f(\Psi, x)$ and L_{eddy} are determined with the aid of the FEM model and stored in the form of characteristic diagrams.

The relation $F(\Psi, x)$ is shown in **Figure 12**. It describes the force F generated depending on the flux linkage Ψ and the armature position x.

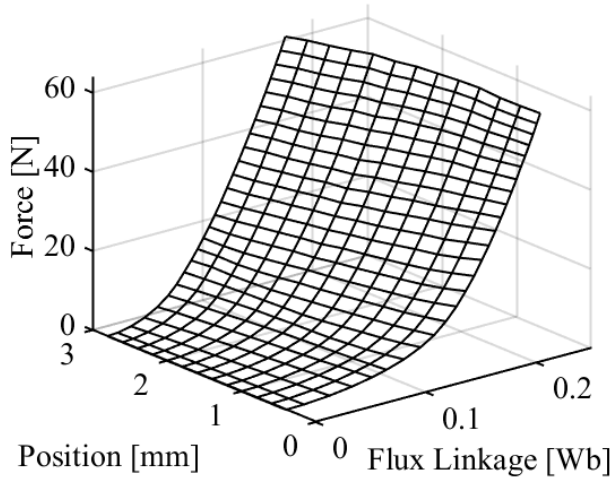

Figure 12: Force F Generated Depending on the Flux Linkage Ψ and the Armature Position x.

The relation $i_f(\Psi, x)$ is shown in **Figure 13**. The characteristic diagram describes the relationship between the field-generating current i_f, the flux linkage Ψ and the armature position x.

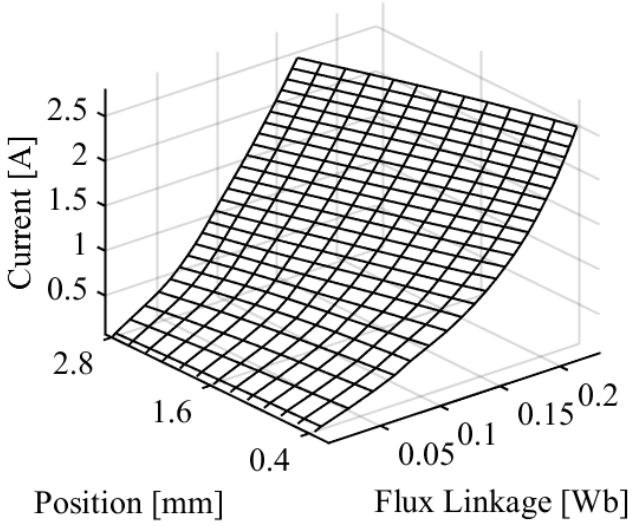

Figure 13: Field-Generating Current i_f, in Dependence of the Flux Linkage Ψ and the Armature Position x.

To evaluate occurring eddy currents, various signals were simulated with different current change rates.

As the focus of this work is on the parameterization of real-time capable models, extensive modeling of the eddy currents, for example using a shell model as shown in [8], is not carried out. Instead, the approach described in **Section 2** is used. A simplified linear dependence between the eddy currents and the induced voltage is assumed.

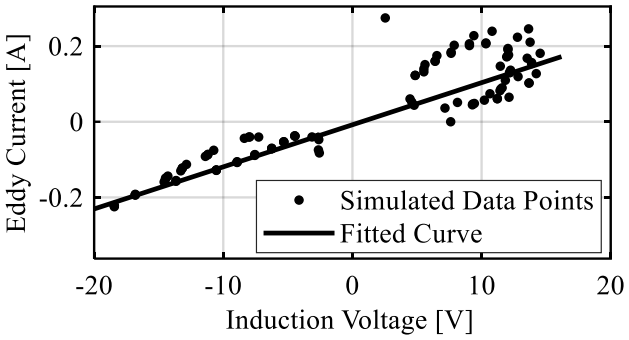

Figure 14: Fit of the Occurring Eddy Currents Depending on the Induction.

Figure 14 shows an example of the eddy currents occurring as a function of the induced voltage for an excitation with triangular current signals of different maximum heights and current change rates. In the investigations, current change rates to a maximum of 125A/s were considered.

As the rate of current change increases, eddy currents increase as well and require a more complex model to describe them. In **Figure 14**, this can be recognized by the fact that the eddy currents scatter further away from the linear regression line with increasing current change rates.

6. VALIDATION

The validation of the new approach for optimizing the initial curve is carried out in two steps. In the first step, the optimized material parameters are used to simulate operating points with the FEM simulation, which were not part of the optimization. The results are then compared with measured data. In the second step, the optimized parameters are used to investigate the dynamic behavior of the solenoid during a ramped excitation. The results of the simulations are compared with those obtained with non-optimized parameters.

First, the results of two FEM simulations with and without an optimized initial curve were compared. **Figure 15** illustrates the force versus stroke at a current of 1.5 A.

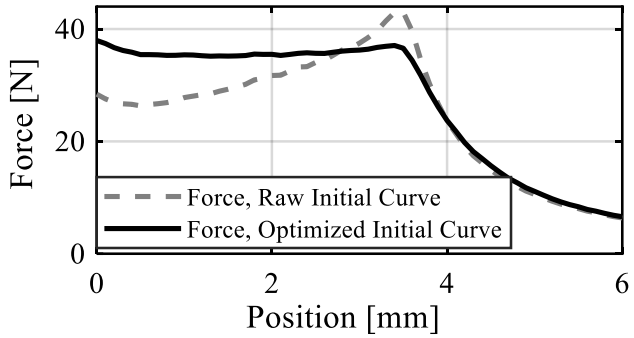

Figure 15: Magnetic Force as a Function of Stroke at a Current of 1.5 A.

The dashed line represents the force, calculated with an unoptimized initial curve. The force progression exhibits poor linearity in the working range of 0.5-2.8 mm. The solid line represents the force characteristic calculated using the optimized initial curve. It is evident, that the linearity within the operating range has been significantly improved after optimization, which is more consistent with the measured characteristics of the actuator.

For further validation, first, the simulated and measured magnetic flux, and subsequently the force is considered.

The magnetic flux at one armature position has been used to determine or optimize the initial curve.

The course and magnitude of the magnetic flux usually changes significantly depending on the armature stroke. To verify the optimized initial curve, the magnetic flux at other positions is simulated and then compared with measured data in **Figure 16**.

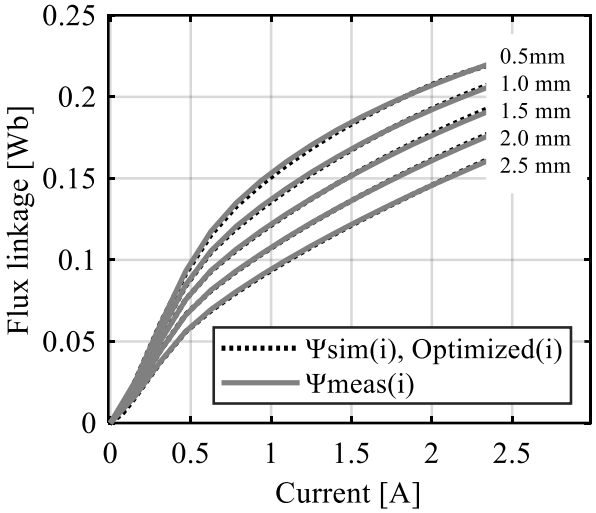

Figure 16: Measured and Simulated Flux using the FEM Simulation with Optimized Initial Curve as a Function of Current for different Strokes.

As can be seen in **Figure 16**, the simulated and measured fluxes are close to each other for all positions. The shape and curvature of the characteristics have been reproduced. The deviation between simulated and measured values increases with increasing excitation.

In Figure 17, the measured magnetic force is compared to the magnetic force calculated by the FEM simulation with an optimized initial curve.

The measurement of the axial force is performed as described in Section 3. The force is plotted at different excitations of 0.5 A, 1 A, 1.5 A, 2 A in the working range of 0.5 to 2.8 mm. The simulated force-stroke characteristics are depicted by marked lines. The measured ones by solid lines. The measured force curves show a hysteretic behavior typical for this kind of solenoid. It can be assumed that the hysteresis is caused by frictional forces acting with the same magnitude in both directions of movement. The force generated by the magnet can therefore be assumed to lie between the upper and lower hysteresis curves.

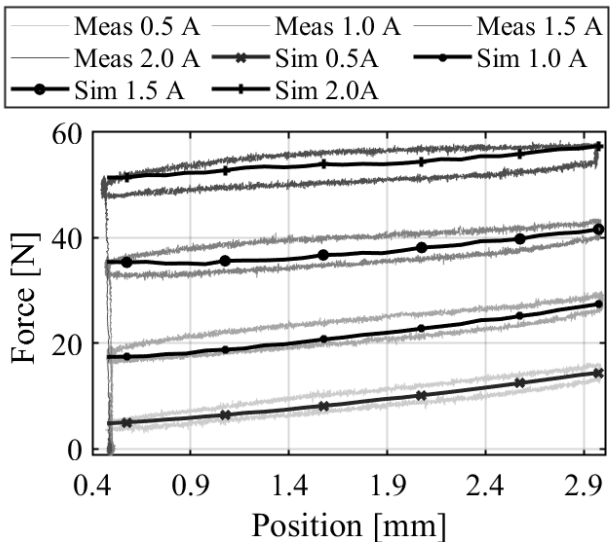

Figure 17: Measured Force and Simulated Force using the FEM Simulation with Optimized Initial Curve.

It should be taken into account that measurement errors in the flux measurement as well as an insufficient quality of the meshing lead to a distortion of the initial curve. These distortions would lead to deviations between simulated and measured force values at operating points not used to optimize the initial curve. In the present case, however, the simulation results agree well with the measurements for all operating points considered. Deviations that affect or offset the flux and force characteristics equally over the entire excitation in all positions cannot be identified by this validation method. If available, a measured initial curve could be used for this purpose.

For a final validation, the dynamic behavior respectively the force build-up of the solenoid during a ramp-shaped excitation with a current change rate of 10 A/s is investigated. For this purpose, the simulation results with and without an optimized initial curve, were compared to a measured force build-up in **Figure 18**.

The solid curve shown in **Figure 18** describes the simulated force with the unoptimized initial curve. The dashed curve describes the simulated force with optimized and the dotted curve the measured force.

The deviation of the simulation with non-optimized parameters is more than 20 N. The large deviation can be explained by the fact that the initial curve used was taken from generally available material data. Changes in the composition and the annealing process can have a significant effect on the magnetic properties and vary from manufacturer to manufacturer and sometimes from batch to batch.

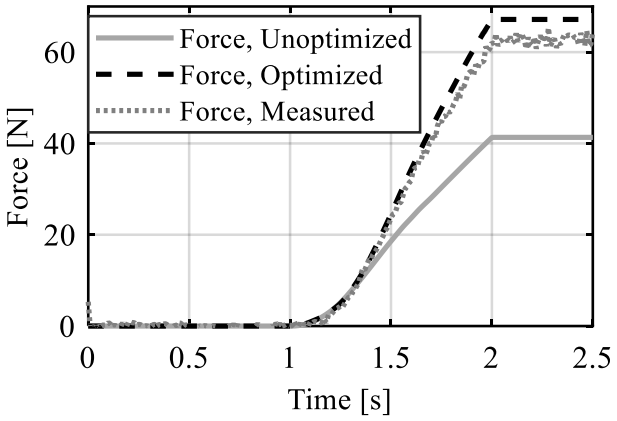

Figure 18: Measured and Simulated Force Build-up of the Solenoid With and Without Optimization.

Simulations based on measured initial curves of the unprocessed material show less pronounced but nevertheless often intolerable deviations as shown in [5].

It can be clearly seen that the simulated force curve with an optimized initial curve is closer to the measured force curve. The remaining deviation is smaller than 3 N and corresponds to the hysteresis of the force characteristics shown in **Figure 17**.

The magnetic and friction hysteresis has not been considered in the modeling. Comparing the measured and simulated force in **Figure 17**, the measured force is lower than the simulated force when the current increases due to the hysteresis. Thus, the simulated (optimized) force shown in **Figure 18** is greater than the measured force by half the hysteresis width. Apart from the expected deviation due to the non-observed hysteresis, the simulation represents the force build-up well.

Therefore, without the knowledge of exact material parameters, the presented method allowed not only to significantly improve the FEM, but also the real-time capable dynamic model.

7. CONCLUSION AND OUTLOOK

In the present work, the simulative parameterization of real-time capable solenoid models was investigated. For this purpose, the structure of the used lumped-parameter model, the FEM model as well as the test rigs for the metrological investigation were described. Subsequently, a new method was presented which makes it possible to determine the material parameters of the magnetic circuit required for the FEM simulation. As validation, the force generated by the magnet at different operating points was simulated with the newly determined material parameters and compared to the measurements. The simulated data agreed well with the measured data. The accuracy of the FEM simulation was significantly improved. With the aid of the improved FEM simulation, the parameters for a real-time model were then derived. Finally, the dynamic behavior respectively the force build-up of the solenoid was considered. It was found that the simulation with optimized parameters showed a smaller deviation from the measured force build-up than the simulation with unoptimized parameters. In planned future work, a hysteresis and an extended eddy current model will be presented that allows better representation for higher current change rates. In addition, the method presented here offers the future possibility of detecting deviations in the material parameters caused by production or variations between batches. These can be taken into account in the simulation of magnetic actuators to improve model accuracy. A more accurate simulative representation of the solenoid would also simplify the adaptation of existing solenoids.

In terms of real-time capable models, more accurate FEM models allow real-time capable solenoid models to be parameterized inexpensively, quickly, and with high accuracy. Such models could then be used for closed-loop control or in soft sensors as well as for condition or power monitoring applications.

NOMENCLATURE

U	Voltage
R	Resistance
i	Current
Ψ	Flux linkage
Θ	Magnetomotive force
w	Number of windings
R_m	Magnetic resistance
F	Force
x	Position
H	Field strength
B	Flux density
μ	Permeability

ACKNOWLEDGEMENTS

This research was funded by Forschungskuratorium Maschinenbau e.V. FKM, grant number 7052200.

REFERENCES

[1] S. Hucko, H. Krampe, and K. Schmitz, "Evaluation of a Soft Sensor Concept for Indirect Flow Rate Estimation in Solenoid-Operated Spool Valves," *Actuators*, vol. 12, no. 4, p. 148, 2023, doi: 10.3390/act12040148.

[2] S. Rosenbaum, *Entwurf elektromagnetischer Aktoren unter Berücksichtigung von Hysterese*. Zugl.: Ilmenau, Techn. Univ., Diss., 2011. Ilmenau: Univ.-Verl. Ilmenau, 2011. [Online]. Available: https://www.db-thueringen.de/receive/dbt_mods_00018835

[3] N. D. Vaughan and J. B. Gamble, "The Modeling and Simulation of a Proportional Solenoid Valve," *Journal of Dynamic Systems, Measurement, and Control*, vol. 118, no. 1, pp. 120–125, 1996, doi: 10.1115/1.2801131.

[4] S. S. Tørdal, A. Klausen, and M. K. Bak, "Experimental System Identification and Black Box Modeling of Hydraulic Directional Control Valve," *MIC*, vol. 36, no. 4, pp. 225–235, 2015, doi: 10.4173/mic.2015.4.3.

[5] Albert Wolfgang Schultz, "Simulationsgestützter Entwurf elektromagnetischer Linearaktoren für fluidtechnische Ventile," p. 119. [Online]. Available: https://d-nb.info/988163764/34

[6] C. Krimpmann, A. Makarow, T. Bertram, I. Glowatzky, G. Schoppel, and H. Lausch, "Simulationsgestützte Optimierung von Gleitzustandsreglern für hydraulische Wegeventile," *at - Automatisierungstechnik*, vol. 64, no. 6, 2016, doi: 10.1515/auto-2016-0017.

[7] R. Keilig, *Entwurf von schnellschaltenden (hochdynamischen) neutralen Elektromagnetsystemen*, 2007. [Online]. Available: https://www.db-thueringen.de/receive/dbt_mods_00010741

[8] E. Kallenbach, R. Eick, T. Ströhla, K. Feindt, M. Kallenbach, and O. Radler, *Elektromagnete: Grundlagen, Berechnung, Entwurf und Anwendung*, 5th ed. Wiesbaden: Vieweg, 2018. [Online]. Available: https://ebookcentral.proquest.com/lib/gbv/detail.action?docID=5214990

[9] R. Boll, *Weichmagnetische Werkstoffe: Einführung in den Magnetismus, VAC-Werkstoffe und ihre Anwendungen*, 4th ed. Berlin, München: Siemens-Aktiengesellschaft, 1990.